Supplementary Material: Efficient shapes for microswimming: from three-body swimmers to helical flagella

Bram Bet,[1,*] Gijs Boosten,[2] Marjolein Dijkstra,[2] and René van Roij[1]

[1]*Institute for Theoretical Physics, Center for Extreme Matter and Emergent Phenomena, Utrecht University, Princetonplein 5, 3584 CC Utrecht, The Netherlands*
[2]*Debye Institute for Nanomaterials Science, Utrecht University, Princetonplein 1, 3584 CC Utrecht ,The Netherlands*

(Dated: November 29, 2016)

DESCRIPTION OF THE ANIMATIONS

In the animations found in the electronic supplementary material, we depict some of the swimmers considered in the main text. For each of these swimmers, the resistance tensor $\mathcal{R}$ is calculated with our numerical model and subsequently the power and the velocities of each swimmer part are calculated. We adjusted the internal velocities of the swimmer such that in every animation, all of the swimmers are swimming at equal average power. Therefore, the fastest swimmer in each animation corresponds to the one with the highest swimming efficiency.

Animation 1 (Fig. 1a) shows three-body swimmers consisting of spheres (red), cubes (blue) and tetrahedra (green), all with maximum arm length $D = 15R$ and amplitude $\epsilon = 6R$, where $\frac{4\pi}{3}R^3$ is the volume of one particle (see main text). We observe that in this regime, the three-tetrahedron swimmer swims the fastest, agreeing with the results of Fig. 4(b) of the main text. Animation 2 shows again three-body swimmers consisting of spheres (red), cubes (blue) and tetrahedra (green) with $D/R = 15$, but now with minimum separation $D - \epsilon$ close to contact. In this case, it is the cube swimmer which swims faster than the three-sphere swimmer, which in turn swims faster than the three-tetrahedron swimmer. This is in agreement with Fig. 4(c) in the main text. Animation 3 and 4 (Fig. 1c and 1d) show a comparison of two three-cube swimmers with $D/R = 10$ and $D/R = 30$ respectively, where the bottom swimmer swims with a square stroke and the top swimmer uses a triangular stroke. We observe that the square stroke is more efficient for $D/R = 10$ while the triangular stroke is more efficient for $D/R = 30$.

Animation 5 (Fig. 1e) shows four different helical flagellum swimmers, all with $L/D = 2.5$, $\ell/R = 11$ and $\rho/R = 0.051$. The motor rotation rate of each swimmer is adjusted such that all four swimmers swim at equal instantaneous power. Note that in this case, the instantaneous power is constant during the stroke and therefore equals the average power. From bottom to top, we show swimmers with shape parameters:

1. $r/R = 0.33$ and $\alpha = 0.87$, corresponding to the shape of E. coli,
2. $r/R = 0.68$ and $\alpha = 0.5$,
3. $r/R = 0.68$ and $\alpha = 0.8$, corresponding to the global maximum in Fig. 4(a) of the main text,
4. $r/R = 3.0$ and $\alpha = 0.75$, the 'wagging tail'-type flagellum corresponding to a local maximum for smaller L/D.

Indeed, we see that the fastest swimmer is the third swimmer, corresponding to the maximum efficiency in Fig. 4(a). Animation 6 (Fig. 1f) shows swimmers with $L/D = 2.5$, $\ell/R = 11$ and $\rho/R = 0.051$, with (from bottom to top):

1. $r/R = 0.33$ and $\alpha = 0.87$, corresponding to the E. coli flagellum shape,
2. $r/R = 0.33$ and $\alpha = 0.5$,
3. $r/R = 1.0$ and $\alpha = 0.8$, corresponding to the flagellum shape of the global maximum for $L/D = 1.0$ in Fig. 4(b) of the main text,
4. $r/R = 4.25$ and $\alpha = 0.75$, the 'wagging tail'-type local maximum.

Comparing with the $L/D = 2.5$ case, the 'wagging tail'-type swimmer (swimmer 4.) now 'finishes' closer to the fastest swimmer, indicating the second local maximum in Fig. 4(b) of the main text. Note that the white line (animation 5) and dot (animation 6) are included to visualize the rotation of the cell body, which is in opposite direction to the rotation of the flagellum. Also, the red arrows indicate the rotation rate of the cell body and flagellum.

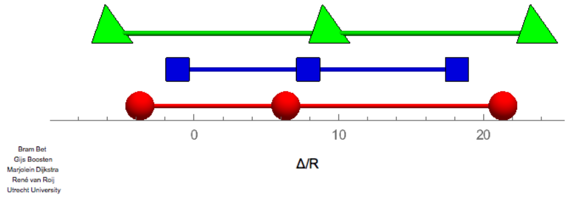

(a) Animation 1: three-body swimmers consisting of spheres (red), cubes (blue) and tetrahedra (green), with maximum arm length $D = 15R$ and amplitude $\epsilon = 6R$. (Multimedia view)

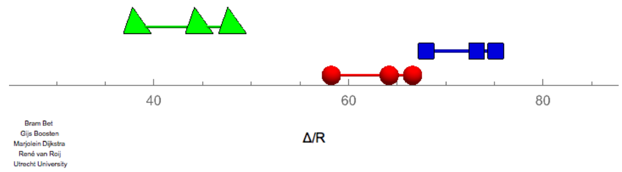

(b) Animation 2: three-body swimmers consisting of spheres (red), cubes (blue) and tetrahedra (green), with $D/R = 15$ and minimum separation $D - \epsilon$ close to contact. (Multimedia view)

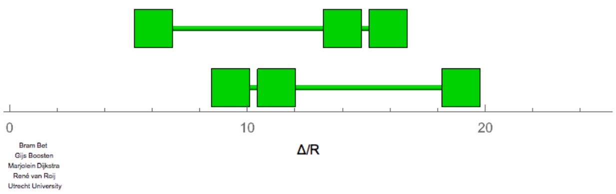

(c) Animation 3: three-cube swimmers with $D/R = 10$, with a square stroke (bottom) and triangular stroke (top). (Multimedia view)

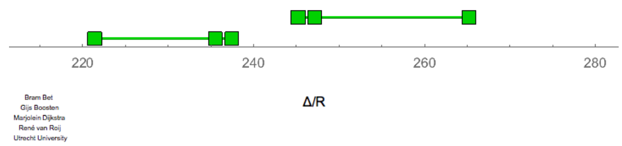

(d) Animation 4: three-cube swimmers with $D/R = 30$, with a square stroke (bottom) and triangular stroke (top). (Multimedia view)

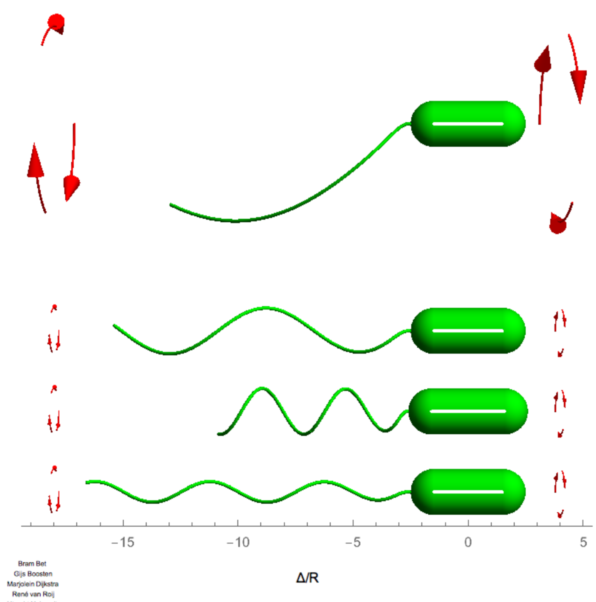

(e) Animation 5: helical flagellum swimmers, with $L/D = 2.5$, $\ell/R = 11$ and $\rho/R = 0.051$, and from bottom to top: $r/R = 0.33$ and $\alpha = 0.87$; $r/R = 0.68$ and $\alpha = 0.5$; $r/R = 0.68$ and $\alpha = 0.8$; $r/R = 3.0$ and $\alpha = 0.75$. (Multimedia view)

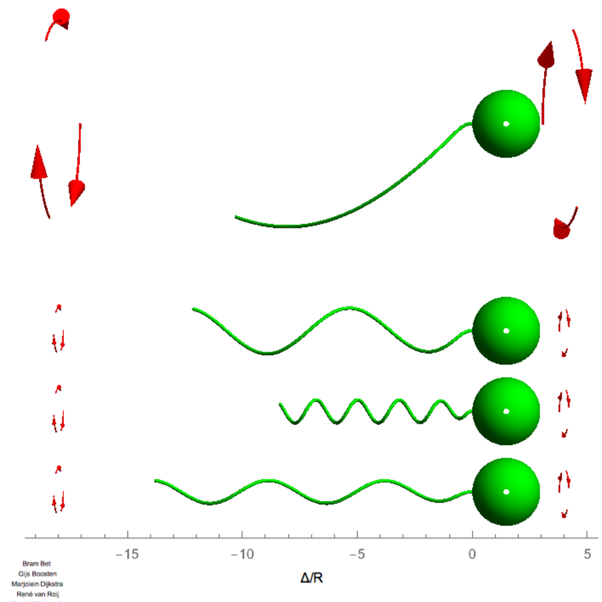

(f) Animation 6: helical flagellum swimmers, with $L/D = 1.0$, $\ell/R = 11$ and $\rho/R = 0.051$, and from bottom to top: $r/R = 0.33$ and $\alpha = 0.87$; $r/R = 0.33$ and $\alpha = 0.5$; $r/R = 1.0$ and $\alpha = 0.8$; $r/R = 4.25$ and $\alpha = 0.75$. (Multimedia view)

FIG. 1: Animations of the swimmers described in the main text.